

## Effect of Number of RF Transmit Channels for RF Shimming in Partial Region

Yukio Kaneko<sup>1</sup>, Yoshihisa Soutome<sup>1</sup>, Hideta Habara<sup>1</sup>, and Yoshitaka Bito<sup>1</sup>  
<sup>1</sup>Hitachi Ltd., Central Research Laboratory, Kokubunji, Tokyo, Japan

### INTRODUCTION

The  $B_1$  inhomogeneity in the human body increases as the strength of a static magnetic field increases. Various multi-channel RF transmission methods for reducing the  $B_1$  inhomogeneity have recently been developed, and RF shimming [1, 2] is used in commercial MRI apparatuses. The impact of the number of RF transmit channels for RF shimming was experimentally and numerically investigated [3, 4]. It was found that a high  $B_1$  homogenization performance is shown in the 2-channel RF shimming, and the performance is limited beyond 2-channel RF shimming, increasing the number of RF transmit channels [4]. These studies showed the effect of RF shimming for the entire region of the torso. The RF shimming for a partial region of the body (regional RF shimming) has also been investigated [5-8]. On the other hand, the effect of the number of the channels for RF shimming for a partial region of the torso in 3T has not yet been investigated. In this study, numerical simulation has been used to investigate the effect of the number of RF transmit channels for regional RF shimming in the 3T torso region.

### METHOD

The effect of the number of RF transmit channels was confirmed using the numerical analysis of the electromagnetic field. The spatial distributions of  $B_1$  in the torso phantom and the human model were calculated, using an electromagnetic simulation tool (xFDTD<sup>®</sup>). The phantom was 300 x 200 x 600 mm in size. The conductivity and relative permittivity of the phantom were 0.60 S/m and 78, respectively. A female model was used as the human model, and the lumbar spine was set at the center of the RF coil. Eight loop-array coil was used for the RF transmission, and RF frequency was 128 MHz. Each loop coil was 265 x 600 mm in size. 2-/4-/8-channel RF shimming were conducted by combining some channels. Figure 1 shows a schematic of the position of the regions used in the RF shimming. The entire region covered the entire torso region along an axial plane. The entire region of the torso phantom was 300 x 200 mm in size, and that of the human model was 400 x 240 mm in size. The partial region was positioned at the lower region of the torso phantom and the human model as shown in Fig. 1. The partial region was 200 x 100 mm in size. The  $B_1$  map data for the entire region or the partial region was used for the optimization of the  $B_1$  homogeneity. The  $B_1$  homogeneity value ( $U_{SD}$ ) was used to evaluate the  $B_1$  inhomogeneity, and  $U_{SD} = \text{standard deviation of } B_1 / \text{average of } B_1$ . The  $U_{SD}$  in the entire or partial region was minimized in 2-/4-/8-channel RF shimming.

### RESULTS AND DISCUSSION

Figure 2 shows the  $B_1$  maps in the cases of RF shimming for the entire region of the phantom. Case (a) represents quadrature (QD) drive, case (b) represents 2-channel RF shimming, case (c) represents 4-channel RF shimming, and case (d) represents 8-channel RF shimming. The  $B_1$  values were normalized with the average of  $B_1$  in case (a). The  $B_1$  map for 2-channel RF shimming is more homogeneous than that for QD. The  $B_1$  maps for the 2-/4-/8-channel RF shimming were almost the same. This is because the shape of the phantom is symmetric and the dielectric property is uniform in the phantom. Figure 3 shows the  $B_1$  maps in the cases of RF shimming for the partial region of the phantom. Case (a) represents QD, case (b) represents 2-channel RF shimming, case (c) represents 4-channel RF shimming, and case (d) represents 8-channel RF shimming. The total RF drive power in all cases of RF shimming was within  $\pm 10\%$  of that in QD. For the 2-channel RF shimming, the  $B_1$  maps are almost the same between the entire and partial regions. For the 4-/8-channel RF shimming, the spatial distributions of  $B_1$  are asymmetric, and the distributions inside the partial region are more homogeneous than that for the 2-channel RF shimming. Figure 4 shows the  $B_1$  homogeneity value ( $U_{SD}$ ) for the phantom and the human model. In the case of RF shimming for the partial region of the phantom, the  $U_{SD}$  decreases for the 2-channel RF shimming compared to the  $U_{SD}$  in QD. The  $U_{SD}$  doesn't change in the 2-/4-/8-channel RF shimming. In the case of RF shimming for the partial region in the phantom, the  $U_{SD}$  decreases, increasing the number of RF transmit channels, and the  $U_{SD}$  in the 8-channel RF shimming is the smallest. In the cases for the human model, the tendency was the same as for the phantom. This result indicates that the effect of multi-channeling beyond 2-channel can contribute to improving the  $B_1$  inhomogeneity in the partial region.

### CONCLUSION

A numerical simulation was conducted to try to determine the effect of the number of RF transmit channels for regional RF shimming in the 3T torso region. The results show that 4- and 8-channel RF shimming can contribute to improving the  $B_1$  inhomogeneity in a partial region.

### REFERENCES

[1] Nistler J et al. ISMRM 2007; 15: 1063. [2] Hajnal JV et al. ISMRM 2008; 16: 496. [3] Childs A et al. ISMRM 2012; 20: 2610. [4] Harvey PR et al. ISMRM 2010; 18: 1486. [5] Ibrahim TS et al. NMR Biomed. 2009; 22: 927-936. [6] van den Bergen B et al. JMRI 2009; 30: 194-202. [7] Bitz AK et al. ISMRM 2009; 17: 4767. [8] Krishnamurthy R et al. ISMRM 2011; 19: 3353.

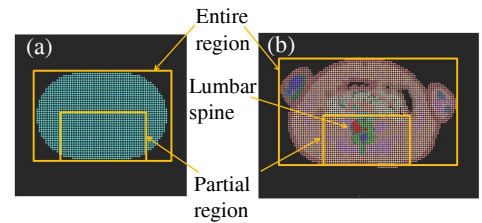


Fig.1 Positions of entire and partial regions used in RF shimming. (a) Torso phantom and (b) human model.

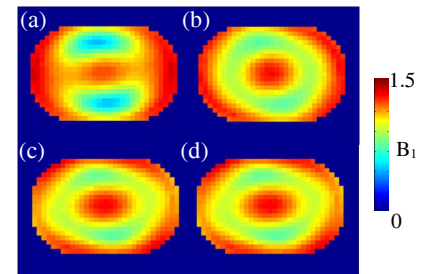


Fig.2  $B_1$  maps in the cases of RF shimming for the entire region of the phantom. (a) QD, (b) 2-channel RF shimming, (c) 4-channel RF shimming, and (d) 8-channel RF shimming.

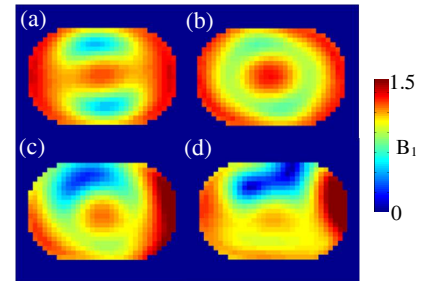


Fig.3  $B_1$  maps in the cases of RF shimming for the partial region of the phantom. (a) QD, (b) 2-channel RF shimming, (c) 4-channel RF shimming, and (d) 8-channel RF shimming.

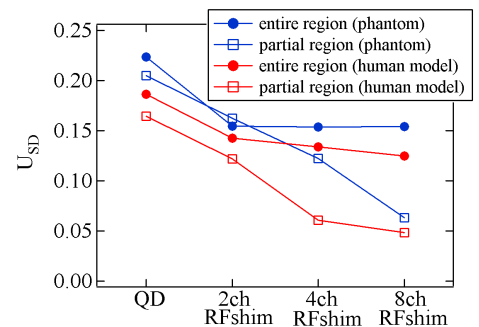


Fig.4  $B_1$  homogeneity in the case of QD and 2-/4-/8-channel RF shimming.